ILC-HiGrade-Report-2013-002

Camera Control for the OBACHT system

Y. Ulrich*, A. Navitski†, L. Steder†, M. Wenskat†

October 2012

Abstract

A high resolution camera and sophisticated illumination system has been mounted in a robot that facilitates the acquisition of images of the inner surface of superconducting cavities, which otherwise are hardly accessible. The OBACHT (Optical Bench for Automated Cavity inspection with High resolution images on short Timescales) system in use at DESY has been optimized for acquisition time and resolution. This note describes the algorithms used to recognize the characteristic welding seam and adjust the focus.

1 Introduction

The "Optical Bench for Automated Cavity inspection with High resolution images on short Timescales" (OBACHT) [1] is a camera system developed for automatic inspection of 9-cell 1,3 GHz SRF-cavity [2] surfaces. Its principle of operation is shown in figure 1.

*yannick.ulrich@physik.uni-hamburg.de
†DESY, Hamburg, Germany

More details are described in [3]: A tube with a camera mounted inside longitudinally slides into the cavity to inspect the surface quality and to detect surface defects. Some aspects of operation are described in this note:

1. Welding seam auto detection: The welding seam is the object of interest because the cavity performance is often correlated with its quality. The algorithm is implemented in LabVIEW.

2. Autofocus: The camera used by OBACHT does not provide an autofocus. However, the camera can be precisely moved longitudinally in the tube by means of a spindle drive, which changes the focus (figure 1). Consequently the autofocus feature can be implemented separately. Moving the camera will cause changes in the contrast of the image.

An OBACHT picture is shown in figure 2. The three light-shaded vertical patterns are the welding seams. The ridge in the centre is the actual welding seam and the lateral lines correspond to the edge of the melting zones. Due to surface treatments they may vary from picture to picture. The image is about $w_m = 12\,\mathrm{mm}$ wide and about $h_m = 9\,\mathrm{mm}$ tall such 1 px equals about 3.5 µm at the equator.

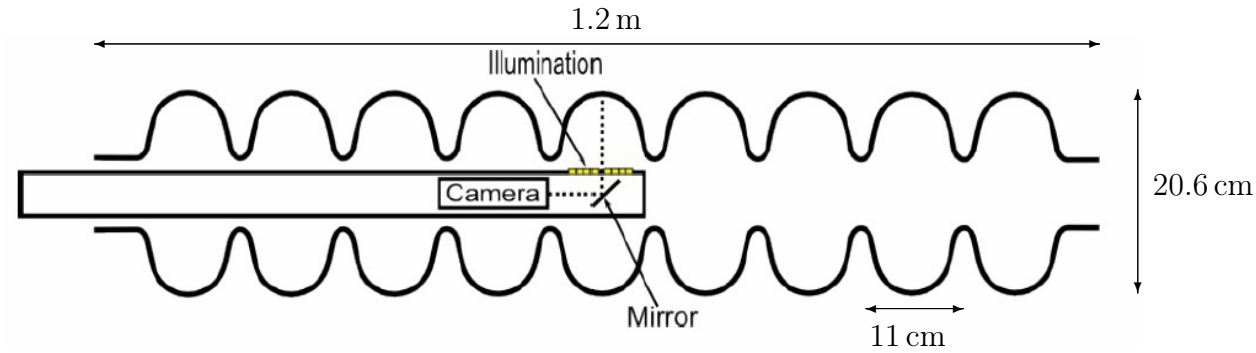

Figure 1: The principle of the OBACHT system [3]: The high-resolution camera is mounted in a tube which can be introduced into the 9-cell cavity. The focus is adjusted by longitudinal movements of the camera inside the tube.

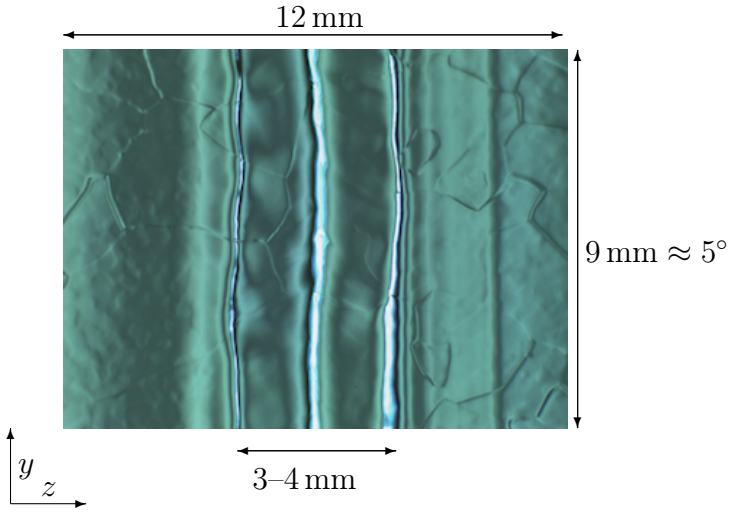

Figure 2: An OBACHT picture of a welding seam

2 Welding seam autodetection

As seen in figure 2 the welding seam and the melting zone are framed by edges with small (ca. 50 µm) lateral variations. The welding seam can be detected as a variation in the intensity pattern. This variation is searched for as a considerable increase in the gradient:

$$G(z, y) = I(z, y) - I(z + 1, y)$$

where G is the gradient and I the intensity image which is calculated using the standard grayscale weighting [4] from LabVIEW:

$$I = 0.3R + 0.59G + 0.11B \tag{1}$$

The grayscale is measured on the scale that varies from 0 to 255.
A typical value for gradient between the background (90) and the welding seam (230) is $10\,\mathrm{px}^{-1}$.
G is calculated for three pixel rows which are effectively perpendicular to the welding seam as can be seen in figure 2. This is approximately the case for all OBACHT picture due to the nature of the image recording. Rows at three coordinates (in this case $y_1 = 500\,\mathrm{px}$, $y_2 = 1000\,\mathrm{px}$ and $y_3 = 1500\,\mathrm{px}$) are evaluated. The y-coordinate is related to the ϕ-coordinate and the z coordinate corresponds to the longitudinal axis of the cylindrical cavity coordinate system described in [5].
These y-rows are marked in figure 3. The gradient along these rows is displayed color-coded in figure 4(a) where the peaks correlate with the welding seams. A lower and an upper threshold t_1 and t_2 are defined to extract the features of the image. From all remaining peaks in each row shown in figure 4(b) the mean position of the first and the last one is calculated. The final output for the seam position is the mean of the peaks from each row.

The algorithm could be modified to detect tilted seams. An example for a tilted seam is shown in figure 5. In the scatter plot is indicated where the welding seam is supposed to be.

2.1 Implementation in LabVIEW

A LabVIEW-file is called virtual instrument (VI). A so-called SubVI is a procedure called by another VI for a specific task. VIs have input and outputs to redirect information from one VI into another. Almost every VI has the input `error in` and the output `error out` used to ensure the user is informed about an occurring error. They also ensure the correct order of execution.
The welding seam auto detection is implemented in `OBACHT_WeldingDetection.vi`.
This VI performs the described algorithm `N` times. It takes an image using `OBACHT_camera_save picture.vi`. Then the saved images are read and the edge detection algorithm from National Instruments is applied to an array of predefined horizontal lines. A threshold is applied to every row. The mean of the first and the last peak gives the value where the welding seam is assumed in this row. After averaging all rows, the pixel offset, the distance from the left corner of the picture to the seam in pixel, is transformed into a millimeter offset:

$$\texttt{millimeter offset} = \frac{w_m}{\texttt{image width}} \cdot \left(\texttt{pixel offset} - \frac{\texttt{image width}}{2} \right)$$

The axial motor adjust the position by `millimeter offset`
The `OBACHT_WeldingDetection.vi` requires the following inputs which are displayed in figure 6:

- `hACam`: ID of the unique camera instance provided by the camera API (application programming interface) to identify the camera.
- `N`: Number of iterations (default: 2)
- `error in`: Input error
- `Operation information`: Operation information
- `error out`: Output error

2.2 Conclusion on the welding seam autodetection

The welding seam auto detection finds the welding seam in about five seconds and can be used to automate the whole positioning procedure for OBACHT. Sometimes problems with the edge detection occur caused by noise in the image. In these cases a manual correction is needed. Another possibility might be moving a few millimeters with the axial motor before restarting the detection which changes the shadows on the surface.

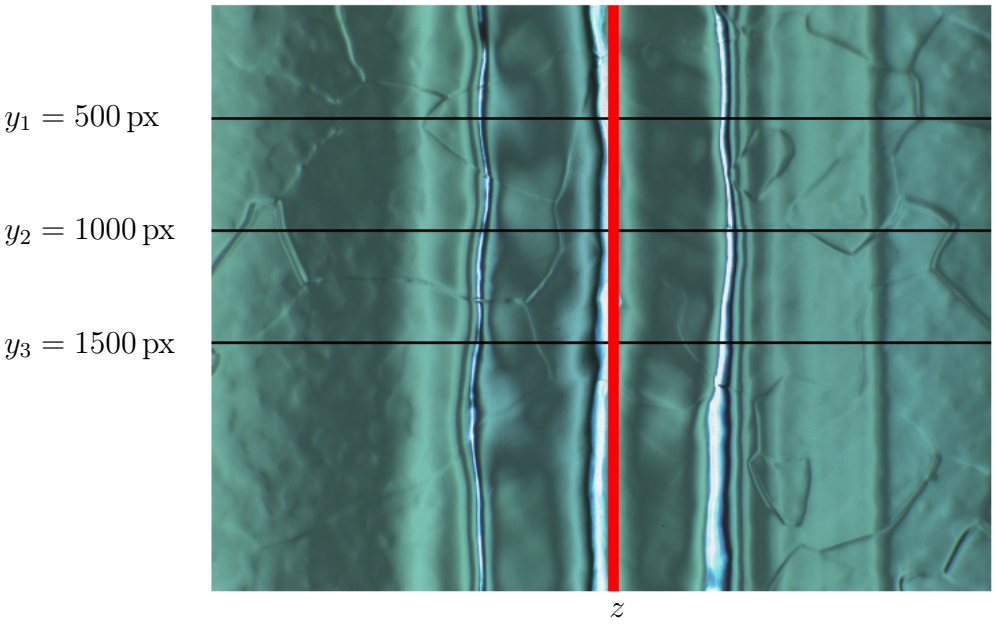

Figure 3: A picture of the welding seam with the three rows y_1, y_2 and y_3 marked. The red vertical line Δz marks the result of the welding seam autodetection. The y-axis of the pictures corresponds to the cavity's ϕ-coordinate [5].

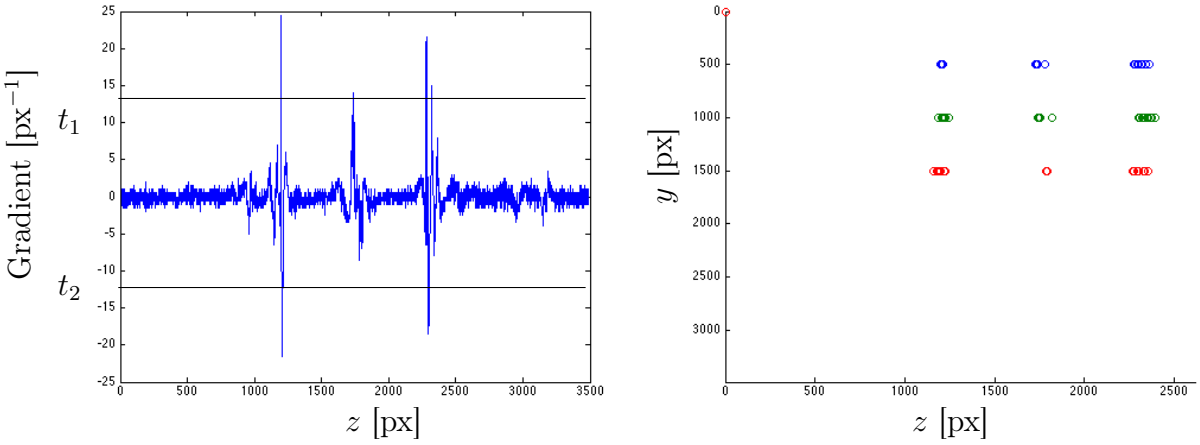

Figure 4: (a) Gradient vs. z-position in pixel. Overlay of all gradients) and both thresholds t_1 and t_2
(b)y-position vs. z-position of all elements outside thresholds

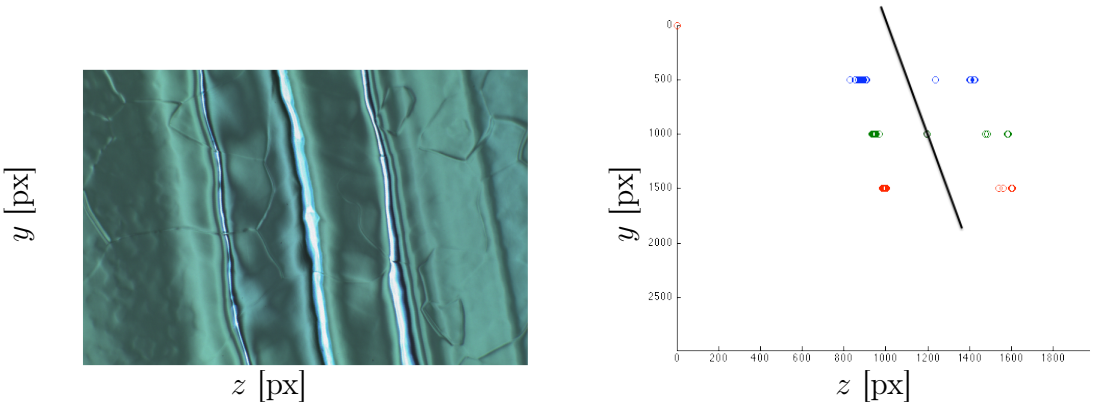

Figure 5: Example of a tilted cell (left) and the resulting threshold pattern on the right.

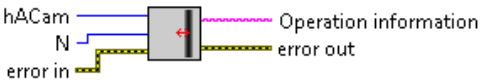

Figure 6: Connections for `OBACHT_WeldingDetection.vi`

3 Autofocus

With a depth of focus of 51 µm the observed variations of depth of 300 µm at the welding seam cannot be captured with uniform constrast. A representative region of interest (ROI) needs to be choosen. Inside this region the variations are explicitly recognized by varitions of the focus.
Numerous autofocusing algorithms were tested at DESY by the Summer Student Raquel Gómez Ambrosio [6]. One of them is using the gradient of the intensity distribution of the image which lies between 0 and 255. It is assumed that the summed gradient $\Sigma|G|$ which can be calculated using a LabVIEW implemented function is a measurement for the contrast of a picture. The larger $\Sigma|G|$ the sharper the image. In figure 7 two welding seam pictures are shown. The corresponding $\Sigma|G|$ values are:

$$\begin{aligned} \Sigma\,|G_a| &= 277\,\mathrm{px}^{-1} \\ \Sigma\,|G_b| &= 312\,\mathrm{px}^{-1} \end{aligned} \tag{2}$$

The z-coordinate describes the camera's position relative to the mirror. The camera is controlled by a stepping motor. 75 focus motor steps corresponds to one DOF. The DOF of the camera is typically set to 51 µm [3] but other values may be chosen.
Multiple pictures with different position and hence different focal planes of the camera are taken. For each picture the $\Sigma|G|$ value is calculated. The peak value of a fitted Gaussian function to the $\Sigma|G|$ can be assumed as the best focus values. An example is shown in figure 8.

(a)

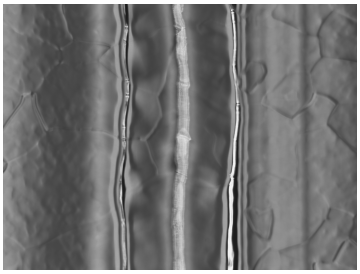

(b)

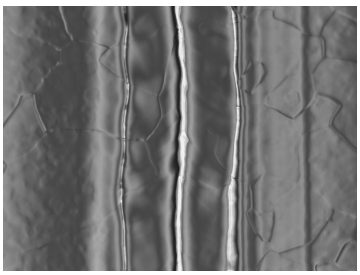

Figure 7: (a) Blurred seam picture(b) same picture with better contrast

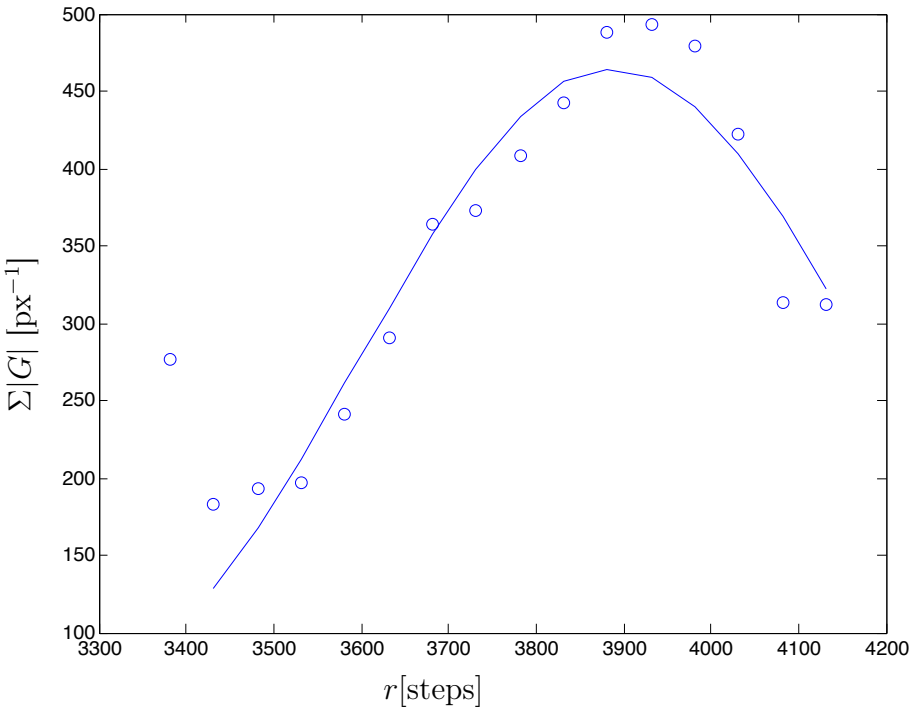

Figure 8: Summed gradient $\Sigma|G|$ over focal distance r in steps of the focus motor. The data is depicted by points, while the Gaussian fit is shown as solid line.

If $\Sigma|G|$ is only calculated for regions with slow variation of distance (eg. 150px wide columns) instead of the entire image, the focus position can be plotted as a function of the image's x axis as shown in figure 9. Assuming the focus position z correlates with the surface topology, this can be used to determine the quality of the autofocus. In figure 9 variations of $\pm 200\,\mu m$, which may not seem unreasonable in view of expected slight variations of the welding seam.

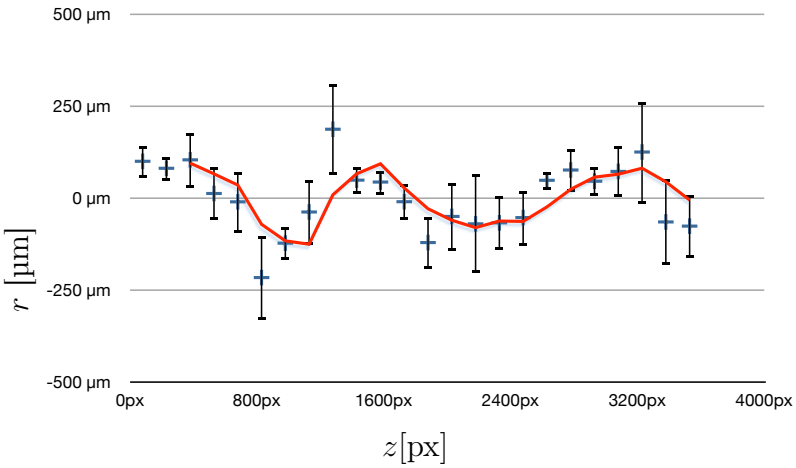

Figure 9: Focus position vs. image's z axis

3.1 The focus table

During the procedure the measured values (4 position along the inner circumference per cell) are saved to interpolate between them in order to extract values for each of the measurement points. This file is called `focustable.txt` and is built following a specific syntax which is displayed below:

```
[CAVITYNAME];[INSPECTION NUMBER];;;
E1;[focus value for E1 at 0 deg];[90 deg];[180 deg];[270 deg]
...
E9;[0 deg];[90 deg];[180 deg];[270 deg]
I1;[0 deg];[90 deg];[180 deg];[270 deg]
...
I10;[0 deg];[90 deg];[180 deg];[270 deg]
```

`En` encodes the n-th equator and `In` the n-th iris.
For the interpolation it is assumed that the cavity's shape is in first order circular so that the focus motor positions can be calculated as linear interpolation of the measurements taken at every 90 degrees.

3.2 Calibration

The focus motor has no end switches that could be used for an absolute position reference. If the operator turns the controller off and back on, the controller is auto calibrated

to zero. To get reproducible results, the values in the focus table are relative to the focus value used at the main coupler [5]. Therefore the autofocus must be applied to the main coupler first and initially to reset the system.

3.3 Implementation in LabVIEW

In figure 10 a code example from the main VI, `AUTOFOCUS.vi`, is shown to visualize the schematics of the LabVIEW algorithm.

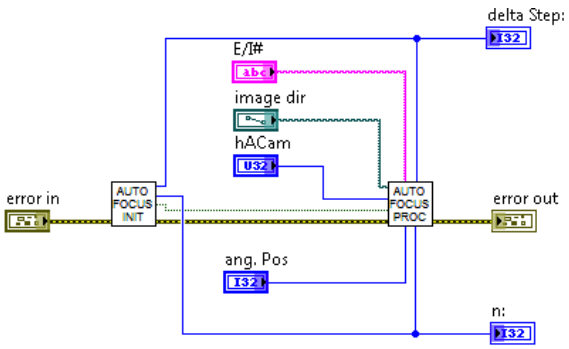

Figure 10: An example from `AUTOFOCUS.vi`

The whole autofocus procedure contains two main parts: Measuring the focus value for certain positions and interpolating for all other positions. The autofocus is used every 90 degrees and the program will interpolate linearly between the measured focus values. In figure 11 a flowchart of the complete autofocus algorithm is shown.

3.3.1 `AUTOFOCUS.vi`

This VI (see figure 10) measures the focus value at a certain position. It will call a SubVI `AUTOFOCUS_init.vi` which is the user interface (UI). The information received from the UI will be transmitted to the `AUTOFOCUS_processing.vi` which manages the autofocus procedure.
In the following, the VI - visible in figure 12 - is explained in detail:

- `E/I#`: Name of the actual cell (E=Equator, I=Iris, MC=main coupler) for identification
- `image dir`: The path to directory for saving the images
- `hACam`: ID of the unique camera instance
- `error in`: Input error
- `ang. Pos`: Angular position in cavity coordinates
- `error out`: Output error

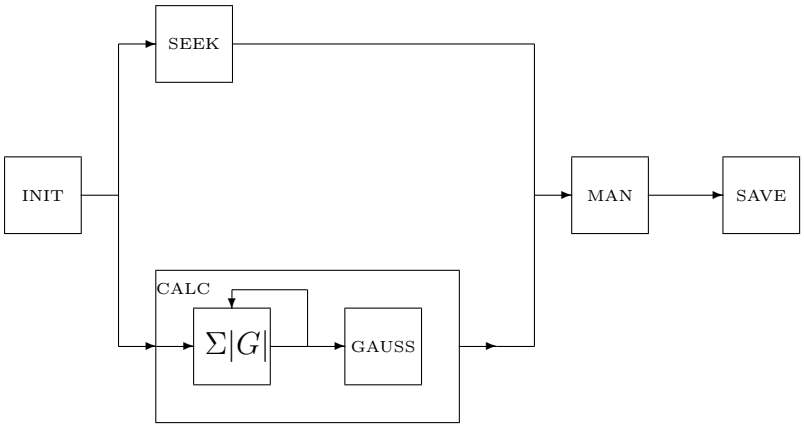

Figure 11: After initiation (INIT), the image taking procedure (SEEK) and the analysis procedure (CALC) are called simultaneously to speed up the procedure. Finally, an option for manual correction (MAN) and the saving (SAVE) are called.

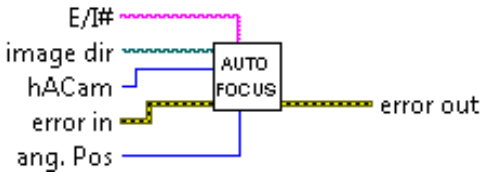

Figure 12: Connections for `AUTOFOCUS.vi`

3.3.2 `AUTOFOCUS_init.vi`

This VI is the user interface (UI) of the autofocus and in the flowchart displayed as INIT. It uses a `while`-loop which is stopped when the user clicked either cancel or start. Its connections can be seen in figure 13 and are explained below:

- `error in`: Input error
- `Number of images`: Number of images to take (default: 20)
- `Step size`: Focus motor distance between two images (default: 20)
- `Start autofocus`: Is set through UI button "Start"
- `error out`: Output error

3.3.3 `AUTOFOCUS_processing.vi`

This VI will process the user input and the autofocus.
If the user does not press start nothing will happen and the procedure will quit. Other-

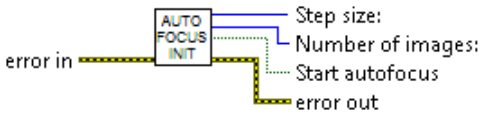

Figure 13: Connections for `AUTOFOCUS_init.vi`

wise the following sequence is called.

1. The global variables by `images2analyse` are reset.
2. The seek sequence (`seek.vi`) and the analysis VI (`calculateFocusGRAD.vi`) are called simultaneously.
3. The user is asked, whether the image is sharp. Otherwise the VI opens a manual controller (`FocusMotorPositioning.vi` is called).
4. If the autofocus is applied to the main coupler, it will just set the focus motor to zero as reference for the next steps. Otherwise it will read the focus table, find the appropriate cell in it by using the values of `E/I#` and `angular position` and replace it with the value just measured.

In figure 14 the connections explained below are shown.

- `delta Step`: Focus motor distance between two images (default: 20)
- `E/I#`: Name of the actual cell (E=Equator, I=Iris, MC=main coupler) for unique identification
- `image dir`: The mandatory path to directory for saving the images
- `hACam`: ID of the unique camera instance
- `start`: True, if the autofocus is started
- `error in`: Input error
- `Angular position`: Angular position in cavity coordinates
- `n`: Number of images to take (default: 20)
- `error out`: Output error

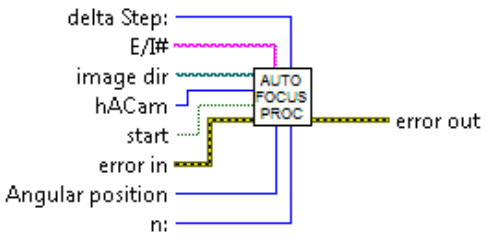

Figure 14: Connections for `AUTOFOCUS_processing.vi`

3.3.4 `calculateFocusGRAD.vi`

This VI runs simultaneously with the image taking VI. In the flowchart it is called CALC. `seek.vi` takes pictures and informs the analysis VI if they are saved.
If new images are available, they are loaded and submitted to a edge detection ($\Sigma|G|$). To the set of $\Sigma|G|$ a Gaussian-peak-fit is applied. The peak value is returned in `best focus position`.

In figure 15 the connections of this VI are shown:

- `# of images`: Number of images to analyze
- `error in (no error)`: Input error
- `best focus position`: The value selected by the user
- `error out`: Output error

Figure 15: Connections for `calculateFocusGRAD.vi`

3.3.5 `gaussian-fit.vi`

This VI (GAUSS) is a Gaussian fitting function with outlier recognition and removal. In order to eliminate these outlying points there are two different ways available: A gradient method and a difference method. The gradient method searches for local fluctuations.The next step is applying the Gaussian fit again on the filtered data in order to get the values for the best focus.
The connections of this VI are displayed in figure 16 and are explained below:

- `X`: Array of x-values
- `Y`: Array of y-values

- `gaussian fit`: A plot that shows the original data, the pre-Gaussian, the corrected data and the Gaussian fit.
- `best focus position`: The peak of the Gaussian fit.

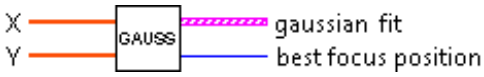

Figure 16: Connections for `gaussian-fit.vi`

3.3.6 `seek.vi`

This VI, in the flowchart referred as SEEK, takes images at different focus motor positions.
At first an offset is calculated, therefore the position z_0 where the motor is right now is saved. The offset is:

$$\texttt{offset} = z_0 - \Delta z \cdot \left\lceil \frac{n-1}{2} \right\rceil$$

where Δz is the distance the focus motor has to move between two pictures. During development $\Delta z = 20\,\text{steps} = 84.68\,\mu\text{m}$. In the following loop the focus motor will be set to the position

$$z_i = \Delta z \cdot i + \texttt{offset}$$

where i is the loop counter. At every position an image is taken and saved as bitmap file. In its filename the focus motor position z_i is saved.
In order to inform the analysis program about the new image to the global variable `images2analyse` the path of the saved image is added.
This VI has the following connections which are also displayed in figure 17:

- `base path`: Path to directory for saving the images
- `hACam`: ID of the unique camera instance
- `Delta z [steps]`: Focus motor distance between two images (default: 20)
- `n`: Number of images to take (default: 20)
- `error in`: Input error
- `z0`: The position where the focus motor started
- `man Abort`: T if user aborts sequence
- `error out`: Output error

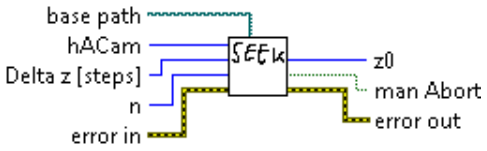

Figure 17: Connections for `seek.vi`

3.3.7 `FocusMotorPositioning.vi`

This VI (MAN) is an UI to replace the hardware controller from the stepping motor of the focus system with an improved and modifiable computer program. It has two buttons for step wise moving and one for target moving. Also the motor speed is settable here. The VI ends when `Save & Done` or `Discard & Abort` is pressed.
Its connections are displayed in figure 18:

- `error in`: Input error
- `z'`: The position where the focus motor is, when the VI is closed
- `error out`: Output error

Figure 18: Connections for `FocusMotorPositioning.vi`

3.3.8 `generate Lookuptable.vi`

This VI (SAVE) adds the focus motor position as a column to the inspection table, a text file where the system parameters for the inspection are saved. At first it checks if the cavity name and inspection number saved in the focus table are identical with those transmitted as parameters. If not, autofocus is not available because the saved information is not valid. Otherwise it applies the following algorithm to every row of the focus table (which contains the value per equator or iris):

- Create a ϕ_n-Array, that has the same size as the z_n-Array:
  Assuming n is the number of elements (the size) of the z-Array. In a `for`-loop ϕ_n is calculated in every iteration like

$$\phi_i = \frac{360\,\mathrm{deg}}{n-1} \cdot i$$

- Find the first row in the inspection table to the corresponding row in the focus table (Example: If the row in the focus table is for the first equator E1, the inspection table is searched for E1 as axial and 0 degrees as angular position)

- Doing a spline interpolation:
  Using a National Instruments example a spline interpolation in 4 degrees- (equator) or 10 degrees-steps (iris) is performed and written to the corresponding cell in the inspection table

The connections of this VI are shown in figure 19:

- `cavity name`: The unique cavity name to identify it
- `inspection #`: The inspection number (as string)
- `Inspection IN`: Inspection table to modify
- `Inspection OUT`: Modified Inspection table

Figure 19: Connections for `generate Lookuptable.vi`

3.4 Conclusion on autofocus

Although the autofocus procedure has smaller teething troubles[1], it may work faster than a human operator in the future. It is able to take and analyze 20 pictures with a $\Delta z = 20\,\text{steps} = 84.68\,\mu\text{m}$ in about three minutes. In order to integrate the autofocus into the OBACHT calibration this time must be reduced. This could be done by optimizing process parameters. Reducing the number of pictures to find the peak position in the standard-deviation-over-focal-distance-plot can save time. A nested intervals algorithm could be an even faster solution. Another possibility to reduce the processing time is to increase the motor speed of the focus motor.

[1] Sometimes the peak of the Gaussian fit could not be calculated

4 Summary

The welding seam autodetection may speed up OBACHT's positioning procedure if the thresholds are set in a way that the illumination is not causing problems to determine the peaks. The seam detection ensures a central position of the seam and can be able to directly detect a non-vertical welding seam, which can either be caused by a non-perfect alignment of camera and cavity or a problem in the welding process.
The autofocus procedure also simplifies the calibration procedure performed before the OBACHT picture taking process. If it is possible to optimize the time consumption of the algorithm, it could be even used during the picture taking. In this case a human operator controlling the focus settings during the whole measurements lasting ten hours would not be necessary any longer.

References

[1] M. Lemke et al., *OBACHT - Optical Bench for Automated Cavity Inspection with High Resolution on Short Time Scales*, ILC-HiGrade-Report-2013-001

[2] C. Adolphsen, M. Barone, B. Barish, K. Buesser, P. Burrows, J. Carwardine, J. Clark and Hélèn. M. Durand *et al.*, "The International Linear Collider Technical Design Report - Volume 3.I: Accelerator & in the Technical Design Phase," arXiv:1306.6353 [physics.acc-ph].

[3] S. Aderhold *"Study of field-limiting defects in superconducting RF cavities for electron- accelerators "* PhD thesis to be published 2013.

[4] Poynton C. 1996. A technical introduction to digital video. New York: John Wiley & Sons.

[5] S. Aderhold, E.Elsen, F. Schlander, L. Steder, *A Common Cavity Coordinate System*, ILC-HiGrade-Report-2011-003 (2011)

[6] Raquel Gómez Ambrosio. *Autofocus System Implementation for Optical Inspection of Superconducting Cavities*. 2010.